Dalton Transactions

Accepted Manuscript

ROYAL SOCIETY OF CHEMISTRY

www.rsc.org/dalton

Dalton Transactions

COMMUNICATION

Dielectric response and anhydrous proton conductivity in a chiral framework containing a non-polar molecular rotor

Received 00th January 20xx,
Accepted 00th January 20xx

DOI: 10.1039/x0xx00000x

www.rsc.org/

Shan-Shan Yu,[a] Shao-Xian Liu,[a] Hai-Bao Duan,*[a,b]

Herein, we report a chiral 3D framework with the formula $[Co(HPO_3)_2][H_2DABCO]$ (DABCO = 1,4-diazabicyclo[2.2.2]octane). This compound exhibits two distinct dielectric anomalies, attributed to the transfer of protons between non-polar DABCO and the inorganic framework and the in-plane oscillatory fluctuation of the DABCO molecule, respectively. It also exhibits proton conductivity under high-temperature anhydrous conditions.

Hydrogen bonding can be employed as a tool for realizing dynamic motion of protons, in which intermolecular proton transfer plays an important role in casing considerable dielectric response and relaxation ferroelectricity. For example, during ferroelectric and antiferroelectric transitions, squaric acid[1] as well as monovalent salts of 1,4-diazabicyclo[2.2.2]octane (DABCO) with tetrahedral anions[2] exhibit high dielectric susceptibility and high electric polarization, respectively. For the transfer of protons in organic solids, the crystal exhibits a significant dielectric response along the supramolecular hydrogen bonding chain, indicating that in response to an applied electric field, protons become mobile and permit the polarization reversal of the chains.[3] Typically, a DABCO molecule is utilized for the construction of a molecular motor; it possesses two proton-accepting nitrogen sites with pK_{a1} = 8.82 and pK_{a2} = 2.97, respectively, and three ionization states.[4] The proton between these two nitrogen sites is ordered in the ferroelectric phase, which will afford long-range dipole arrangement.[5]

On the other hand, it is well known that there is potential for controlling dielectric and optoelectronic phenomena in the ordered arrays of mesoporous materials.[6] Basically, the dielectric response of those materials is due to the rotational or hopping movement of dipolar molecules or ions.[7] Although the rotation of the dipolar motor is common in metal–organic frameworks and organosilicas, there are no examples of inorganic microporous frameworks containing a non-polar rotor exhibiting a dielectric response. Meanwhile, a three-dimensional (3D) crystal lattice of inorganic frameworks can provide well-designed pores for the conduction of protons. The interaction between the pores and guest molecules,[8,9] such as hydrogen bonding and weak coulombic interaction, may contribute to the introduction of guest as media into the pores for the conduction of protons.[10]

In this study, we introduced non-polar DABCO into the 3D crystal lattices as the guest molecule and obtained a chiral 3D framework with the formula $[Co(HPO_3)_2][H_2DABCO]$ (**1**). To the best of our knowledge, for the first time, we present a 3D framework that contains a non-polar molecule exhibiting a two-step dielectric response and intrinsic proton conductivity under high-temperature anhydrous conditions.

Crystals of **1** were synthesized by treating hydrated cobalt chloride ($CoCl_2·6H_2O$) with phosphorous acid (H_3PO_3) and DABCO in DMF (see supporting information). The synthesis is similar to that reported by Su and coworkers.[11] By the comparison of the power X-ray diffraction (PXRD) pattern for the as-prepared sample with that simulated at room temperature, the position of the main diffraction peak did not change, indicative of the phase purity of the as-prepared sample (Figure S1). The thermal stability of **1** was evaluated by Thermogravimetric (TG) analysis (Figure S2). Compound **1** exhibits a gradual weight loss at 200–600 °C (35.40%), attributed to the removal of the DABCO molecule (the calculated weight loss for the complete removal of DABCO molecules was 34.2%). After the loss of DABCO molecules, **1** started decomposition.

The crystals of **1** at room temperature belonged to the chiral space group $P2_12_12_1$. The lattice parameters were very similar to a previously reported compound.[11] The Co–O–Co bond length was similar to those of other cobalt-based phosphates.[12] Compound **1** exhibited a 3D chiral helical framework. In an asymmetric unit, one crystallographically independent Co^{2+} and two different P^{3+} centers were observed. Each Co^{2+} was tetracoordinated to four O atoms, forming a tetrahedron. Each P atom exhibited order at room temperature. The distance between P and O atoms ranged from 1.512 to 1.524 Å. The existence of the P–H bond by confirmed by IR spectroscopy (Figure S3) and other reported compounds.[13] The locations of the protons in phosphite were also confirmed by the

[a] School of Environmental Science, Nanjing Xiaozhuang University, Nanjing 211171,, P.R.China
[b] Department of Chemistry and Biochemistry, University of California, Los Angeles, California 90095-1569, United States

†Electronic Supplementary Information (ESI) available: experimental details, additional figures, power XRD and TG curves. For ESI or other electronic format See DOI: 10.1039/x0xx00000x

bond distances of the P and O atoms. The P–OH and P=O distances ranged from 1.55 to 1.75 Å and 1.50 to 1.51 Å, respectively. Two chiral nanometer-sized negative cavities were formed by alternating CoO_4 and HPO_3 units, with the small one being ca. 6.18 Å (Figure 1a). The larger one was an irregular elongated cavity (Figure S4). For charge compensation, the DABCO molecules were deprotonated and located in chiral cavities. Notably, a line-shaped hydrogen bonding chain was observed between dipronated H_2DABCO^{2+} and phosphite (with hydrogen bonding parameters: $d_{O(1)\cdots N(1)ii}$ = 2.569 Å, $d_{O(1)\cdots H(1)ii}$ = 1.663 Å, ∠N(1)–H(1)^{ii}···O(2) = 176.06°; $d_{O(6)\cdots N(2)i}$ = 2.76 Å, $d_{O(6)\cdots H(2)i}$ = 1.686 Å, ∠N(2)–H(2)^{i}···O(6) = 166.58°, symmetric code: i = 0.5 + x, 1.5 + y, 1 − z; ii = 2 + x, −0.5 + y, 0.5 − z) (Figure 1b). From the view of the crystal structure, **1** was observed as an ideal amphidynamic crystal, requiring architectures with free volume and volume-conserving process.[14] Inorganic phosphite frameworks provide a rigid lattice and large free space; The DABCO molecules could be rotate along the hydrogen-bonding chain direction (Figure 1c). Furthermore, interionic proton hopping was possible to observed between the observed H_2DABCO^{2+} and the negative framework.

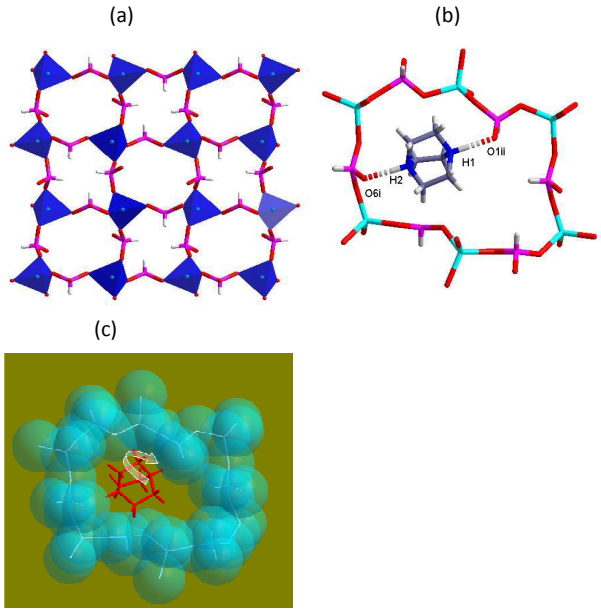

Figure 1 (a) 3D framework structure of **1** along the *a* axis; (b) Hydrogen bonding interaction between DABCO and the framework, and (c) Magnified image of the DABCO rotator in the crystal, indicated by a red stick, and the rigid lattice illustrated in the space filling model.

Dynamics of **1** can be investigated by dielectric measurements because dielectric response can be affected by thermally activated order or disorder transition of the protons within the hydrogen-bonding chain. Figures S5 and S6 show the frequency dependence of the real part of dielectric permittivity (*ε′*) and dielectric loss tan*(δ)* = *ε″*/*ε′* of **1**, respectively, at 40–120 °C and at frequency ranging from 1 to 10^6 Hz. At room temperature, the magnitude of *ε′* was 6–10, indicative of negligible frequency dependence in the kilo- and megahertz-frequency range; this value is characteristic of typical non-polar dielectrics (Figure S7). Unfortunately, it is difficult to analyze the frequency dependence of permittivity because a strong low-frequency dispersion of *ε′* and tan*(δ)* is observed with increasing temperature. Figure 2a shows the dielectric relaxation spectra of **1**, which is transformed into electric modulus spectra by using Eq.(1).

$$M'(\omega) = \frac{\varepsilon'}{\varepsilon'^2 + \varepsilon''^2} \qquad M''(\omega) = \frac{\varepsilon''}{\varepsilon'^2 + \varepsilon''^2} \quad (1)$$

By using the dielectric modulus, the contribution from conductivity effects is enhanced. Another advantage arises from the fact that electrode polarization and the space charge injection effect can be eliminated at low frequency. A two-step dielectric response was clearly observed in the *M″-f* plot. For investigating the mechanism of this two-step dielectric response, the temperature-dependent *ε′* and *ε″* at selected ac electrical field frequency is shown in Figure 2b and 2c. From these figures, the *ε′* and *ε″* values clearly exhibited two distinct anomalies at temperatures ranging from 30 to 80 °C (first step) and 90 to 140 °C (second step), respectively. The first anomaly exhibited only a small response, with almost no frequency dependency (Figure2b and 2d). It was not related to the symmetry-breaking phase transition, as confirmed by different scanning calorimetry and the temperature-dependent single crystal structure. Thus, the first-step dielectric anomaly can be ascribed to the transfer of protons between non-polar DABCO and the inorganic framework. It is reasonable to regard the relaxation mechanism as quantum mechanical tunneling as the polarity inversion is rapid and the permittivity does not exhibit frequency dependence.[15] In the higher-temperature region (second-step dielectric anomaly), the real part, imaginary part, and modulus increased with temperature and exhibited peaks (Figure 2e). All of them were dependent on the ac field frequency. An in-depth analysis of the *M″*-f plot shows that the amplitude of the peak observed at temperatures ranging between 90 and 140 °C increased with frequency, which is similar to ferroelectric relaxation.[16] However, there is no direct evidence for long-range dipolar order. The relaxation time for the second-step dielectric anomaly at the selected frequency from Figure 2f followed the Arrhenius equation (Eq. 2).

$$\tau = \tau_0 \exp\left(\frac{E_a}{k_B T}\right) \quad (2)$$

Here, τ_0 represents the characteristic macroscopic relation time, E_a is the activation energy or potential barrier required for dielectric relaxation, and k_B is the Boltzmann's constant. The best fits using Eq.(2) gave the following results: $\tau_0 = 1.74 \times 10^{-10}$ s and E_a = 0.82 eV. The results show that the DABCO molecules in the inorganic framework are stationary at temperatures below 90 °C, and at high temperature, they acquire the freedom of reorientation with reasonably large activation energy as compared to that of the organic crystal. The reorientation model was analyzed: if the DABCO cations rotate at 120° along the direction of the hydrogen-bonding chain (C_3 axis), this symmetry-conserving moving model does not change the orientation of the dipole moment; thus, it is dielectric-inactive. Thus, the second dielectric response can be attributed to the in-plane oscillatory fluctuation (libration) around the C_3 axis of the DABCO molecule, which is dielectric-active.

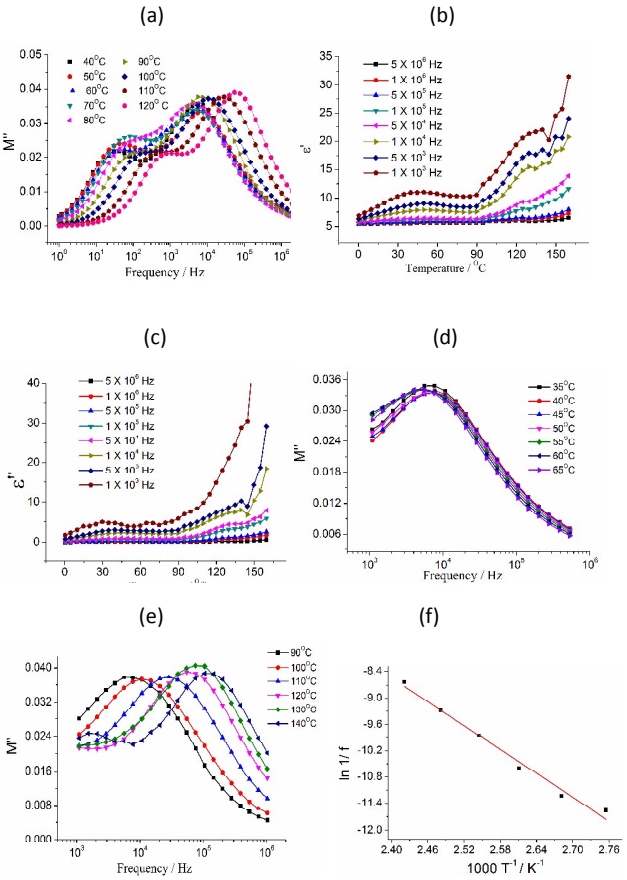

Figure 2 (a) Frequency dependencies of M'' of **1** at 40–120 °C; (b) and (c) Temperature dependencies of ε' and ε'' of **1** at 1 KHz–5 MHz; (d) The first-step dielectric anomaly shows frequency independence of M''; (e) The second-step dielectric anomaly exhibits frequency dependence of M'' and (f) Plots of lnf versus 1/T for the second-step dielectric anomaly.

In the coordinated network of **1**, phosphite groups can serve as desirable sites for the hopping of protons to induce inherent proton hopping. The proton conductivity of **1** was measured by alternating current impedance spectroscopy from 90 to 140 °C under dry N_2, and Figure 3a shows the Nyquist plots. No semicircle was observed for **1** at room temperature under anhydrous conditions, indicative of negligible proton conductivity (Figure S8). The proton conductivity of **1** was determined from the semicircles in the high-frequency regions of Nyquist plots, attributed to both bulk and grain boundary resistance, and the tail in the low-frequency region is due to blocking effects at the electrode interface.[17] The impedance curves can be fitted by the equivalent circuit using the Zview fitting program, where each impedance semicircle can be represented by a resistor R and a capacitor C in parallel. Conductivity increased with temperature. The best fit afforded a proton conductivity of 4.56×10^{-8} S·cm^{-1} at 90 °C and then reached 1.85×10^{-6} S·cm^{-1} at 140 °C, which is less than that of the anhydrous phosphate $[Zn(HPO_4)(H_2PO4)_2](ImH_2)_2$[18] and comparable to that of an imidazole-loaded metal–organic framework.[19] Figure 3b plots the temperature-dependent conductivities σ as lnσ versus 1000/T: a linear relationship was observed at 90–140 °C, and E_a was estimated to be 0.93 eV. This observed conductivity behavior is attributed to the local motion of the proton carrier H_2DABCO^{2+} in **1**, and is confirmed by the second-step dielectric anomaly. However, because of strong host–guest hydrogen bonding interaction and dense packing, the DABCO molecules in **1** were not allowed to freely rotate in the framework, and only local libration moving was permitted. In addition, the long-range hydrogen bonding interaction was absent between DABCO molecules. Thus, the activation energy in **1** is greater than those of the imidazole-loaded metal–organic framework and phosphate, where weak interaction was observed between polar imidazole and the non-polar potential surface.[20]

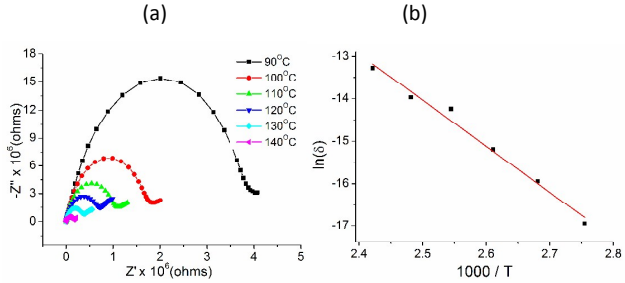

Figure 3 (a) Complex impedance of **1** at selected temperatures and (b) Arrhenius plots of **1** between 90 and 140 °C.

In summary, we reported a chiral 3D framework with dipronated $H_2DABCO_2^+$ in cavities. A line-shape hydrogen bonding chain was observed between $H_2DABCO_2^+$ and phosphite. This compound exhibited two distinct anomalies at temperatures ranging from 30 to 80 °C (first step) and 90 to 140 °C (second step), respectively. The first-step dielectric anomaly was independent of frequency, attributed to the transfer of protons between non-polar DABCO and the inorganic framework. The second dielectric response is attributed to the in-plane oscillatory fluctuation (libration) around the C3 axis of the DABCO molecule. This compound also exhibited a proton conductivity of $>10^{-6}$ S·cm^{-1} at 140 °C without humidity. Our results demonstrated the possibility of obtaining interesting 3D framework materials with interesting dielectric and anhydrous proton conduction properties by fine-tuning host–guest interaction and the pore size for the target proton carrier.

The authors thank the Natural Science Foundation of High Learning Institutions of JiangSu Province and National Nature Science Foundation of China for their financial support (grant No: 13KJD150002, 21201103 and 21301093).

Notes and references

1 Y. Moritomo, Y. Tokura, H. Takahashi and N. Mori, *Phys. Rev. Lett.,* 1991, **67,** 2041.
2 M. Szafranski, A. Katrusiak and G. J. McIntyre, *Phys. Rev. Lett.,* 2002, **89,** 215507.
3 (a) S. Horiuchi, Y. Noda, T. Hasegawa, F. Kagawa and S. Ishibashi, *Chem. Mater.,* 2015, **27,** 6193; (b) M. Morimoto and M. Irie, *Chem. Commun.,* 2011, **47,** 4186; (c) Z. H. Sun, X. Q. Wang, J. H. Luo, S. Q. Zhang, D. Q. Yuan and M. C. Hong, *J. Mater. Chem. C,* 2013, **1,** 2561.

4 D. A. Gunzonas and D. E. Irish, *Can. J. Chem.,* 1988, **66,** 1249.
5 A. Katrusiak and M. Szafranski, *Phys. ReV. Lett.,* 1999, **82,** 576.
6 (a) K. Kim and N. S. Sullivan, *Phys. Rev. B,* 1997, **55**, R664; (b) J.de Jong, M. Ratner and R. S. S. W. De Leeuw, *J. Phys. Chem. B,* 2004, **108**, 2666; (c) R. D. Horansky, L. I. Clarke and J. C. Price, *Phys. Rev. B,* 2005, **725**, 014302; (d) N. Yanai, T. Uemura, W. Kosaka, R. Matsuda, T. Kodani, M. Koh, T. Kanemura and S. Kitagawa, *Dalton Trans.,* 2012, **41,** 4195; (e) M. Usman, S.Mendiratta and K. L. Lu, *ChemElectroChem.,* **2015,** doi:10.1002/celc.201402456.
7 (a) Z. Y. Du, Y. Z. Sun, S. L. Chen, B. Huang, Y. J. Su, T. T. Xu, W. X. Zhang and X. M. Chen, *Chem. Commun.,* **2015,** 51, 15641; (b) P. C. Guo, T. Y. Chen, X. M. Ren, W. H. Ning and W. Q. Jin, *New J. Chem.,* 2014, **38,** 2254; (c) E. B. Winston, P. J. Lowell, J. Vacek, J. Chocholousova, J. Michl and J. C. Price, *Phys. Chem. Chem. Phys.,* 2008, **10,** 5188; (d) W. Zhang, H. Y. Ye, R. Graf, H. W. Spiess, Y. F. Yao, R. Q. Zhu and R. G. Xiong, *J. Am. Chem. Soc.,* 2013, **135,** 5230; (e) R. D. Horansky, L. I. Clarke and J. C. Price, *Phys. Rev. B,* 2005, **72,** 014302.
8 (a) X. Meng, S. Y.Song, X. Z. Song, M. Zhu, S. N. Zhao, L. L. Wu and H. J. Zhang, *Chem. Commun.,* 2015, **51,** 8150; (b) M. Zhu, Z. M. Hao, X. Z. Song, X. Meng, S. N. Zhao, S. Y. Song and H. J. Zhang, *Chem. Commun.,* 2014, **50,** 1912.
9 (a) Q.Tang, Y. W. Liu, S. X. Liu, D. F. He, J. Miao X. Q. Wang, G. C. Yang, Z. Shi and Z. P. Zheng, *J. Am. Chem. Soc.,* 2014, **136,** 12444; (b) P. Ramsswamy, N. E. Wong, B. S. Gelfand and G. K. H. Shimizu, *J. Am. Chem. Soc.,* 2015, **137,** 7640; (c) M. Sadakiyao, T. Yamada and H. Kitagawa, *J. Am. Chem. Soc.,* 2014, **136,** 13166; (d) J.M. Taylor, K. W. Dawson and G. K. H. Shimizu, *J. Am. Chem. Soc.,* 2013, **135,** 1191; (d) W. J. Phang, H. Jo. W. R. Lee, J. H. Song, K. Yoo, B. S. Kim and C. S. Hong, *Angew. Chem. Int. Ed.,* 2015, **54,** 5142; (e) X. J. Li, X. F. Sun, X. X. Li, Z. H. Fu, Y. Q. Su and G. Xu, *Cryst. Growth. Des.,* 2015, **15,** 4543.
10 (a) Y. X. Ye, L. Q. Zhang, Q. F. Peng, G. E. Wang, Y. C. Shen, Z. Y. Li, L. H. Wang, X. L. Ma, Q. H. Chen, Z. J. Zhang and S. C. Xiang, *J. Am. Chem. Soc.,* 2015, **137,** 913; (b) S. C. Liu, Z. F. Yue and Y. Liu, *Dalton Trans.,* 2015, **44,** 12976; (c) S. Horike, D. Umeyama, M. Lnukai, T. Itakura snd S. Kitagawa, *J. Am. Chem. Soc.,* 2012, **134,** 7612.
11 X. C. Liu, Y. Xing, X. L. Wang, H. B. Xu, X. Z. Liu, K. Z. Shao and Z. M. Su, *Chem. Commun.,* 2010, **46,** 2614.
12 (a) Q. R. Ding, L. M. Li, L. Zhang and J. Zhang, *Inorg. Chem.,* 2015, **54,** 1209; (b) L. M. Li, K. Cheng, F. Wang and J. Zhang, *Inorg. Chem.,* 2013, **52,** 5654; (c) E. R. Parnham and R. E. Morris, *J. Am. Chem. Soc.,* 2006, **128,** 2204.
13 (a) X. M. Wang, Y. Yan, J. B. Wu, C. Q. Zhang and J. Y. Li, *CrystEngComm,* 2014, **16,** 2266; (b)G. M. Wang, X. Zhang, J. H. Li, Z. H. Wang and Y. X. Wang, *Inorg. Chem. Commun.,* 2013, **36,** 27.
14 (a) S. L. Gould, D. Tranchemontagne, O. M. Yaghi and M. A. Garcia-Garibay, *J. Am. Chem. Soc.,* 2008, **130,** 3246; (b)T. A. V. Khuong, J. E. Nunez,C. E. Godinez and M. A. Garcia-Garibay, *Acc. Chem. Res.,* 2006, **39,** 413; (c) D. I. Kolokolov, A. G. Stepanov and H. Jobic, *J. Phys. Chem. B,* 2014, **118,** 15978.
15 I. Takasu and T. Sugawara, *J. Phys. Chem. B,* 2004, **108,** 18495.
16 (a) M. Szafranski and A. Katrusiak, *J. Phys. Chem. B,* 2008, **112,** 6779; S. Horiuchi, R. Kumai, Y. Okimoto and Y. Tokura, *Phys. Rev. Lett.,* 2000, **85,** 520; (b) L. E. Cross, *Ferroelectrics,* 1994, **151,** 305.
17 (a) S. Sanda, S. Biswas and S. Konar, *Inorg. Chem.,* 2015, **54,** 1218; (b) P. Ramaswamy, N. E. Wong, B. S. Gelfand and G. K. H. Shimizu, *J. Am. Chem. Soc.,* 2015, **137,** 7640; (c) V. G. Ponomareva, K. A. Kovalenko, A. P. Chupakhin, D. N. Dybtsev, E. S. Shutova and V. P. Fedin, *J. Am. Chem. Soc.,* 2012, **134,** 15640; (d) H. Okawa, M. Sadakiyo, K. Otsubo, K. Yoneda, T. Yamada, M. Ohba and Kitagawa, *Inorg. Chem.,* 2015, **54,** 8529.
18 S. Horike, D. Umeyama, M. Inukai, T. Itakura, and S. Kitawaga, *J. Am. Chem. Soc.,* 2012, **134,** 7612.
19 S. Bureekaew, S. Horike, M. Hiuchi, M. Mizuno, T. Kawamura, D. Tanaka, N. Yanai and S. Kitagawa, *Nat. Mater.,* 2009, **8,** 831.
20 (a) Y. X. Ye, L. Q. Zhang, Q. F. Peng, G. E. Wang, Y. C. Shen, Z. Y. Li, L. H. Wang, X. L. Ma, Q. H. Chen, Z. J. Zhang and S. C. Xiang, *J. Am. Chem. Soc.,* 2015, **137,** 93; (b) S. Horike, W. Chen., T. Itakura, M. Inukai, D. Umeyama, H. Asakura and S. Kitagawa, *Chem. Commun.,* 2014, **50,** 10241.

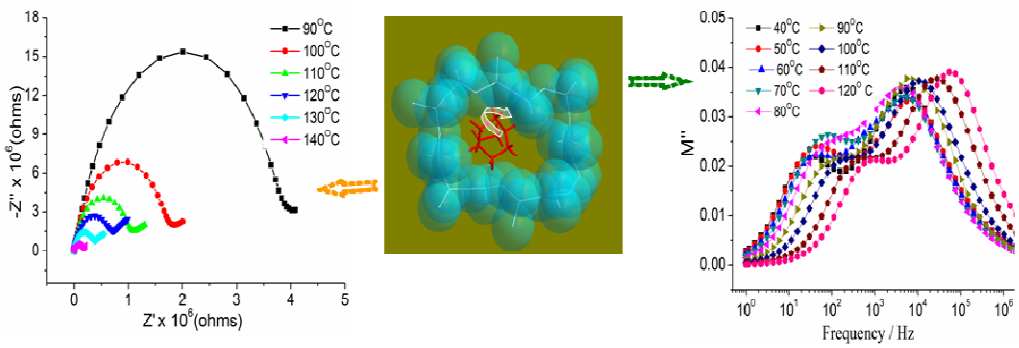

A chiral 3D framework containing nonpolar rotor shows two dielectric anomalies can be serve as proton conductor for high-temperature and anhydrous conditions